Photoreceptor phagocytosis is mediated by phosphoinositide signaling

Debarshi Mustafi,* Brian M. Kevany,* Christel Genoud,‡ Xiaodong Bai,† and Krzysztof Palczewski*,[1]

*Department of Pharmacology and †Center for RNA Molecular Biology, Case Western Reserve University, Cleveland, Ohio, USA; and ‡Electron Microscopy Facility, Friedrich Miescher Institute for Biomedical Research, Basel, Switzerland

ABSTRACT **Circadian oscillations in peripheral tissues, such as the retinal compartment of the eye, are critical to anticipating changing metabolic demands. Circadian shedding of retinal photoreceptor cell discs with subsequent phagocytosis by the neighboring retinal pigmented epithelium (RPE) is essential for removal of toxic metabolites and lifelong survival of these postmitotic neurons. Defects in photoreceptor phagocytosis can lead to severe retinal pathology, but the biochemical mechanisms remain poorly defined. By first documenting a 2.8-fold burst of photoreceptor phagocytosis events in the mouse eye in the morning compared with the afternoon by serial block face imaging, we established time points to assess transcriptional readouts by RNA sequencing (RNA-Seq). We identified 365 oscillating protein-coding transcripts that implicated the phosphoinositide lipid signaling network mediating the discrete steps of photoreceptor phagocytosis. Moreover, examination of overlapping cistromic sites by core clock transcription factors and promoter elements of these effector genes provided a functional basis for the circadian cycling of these transcripts. RNA-Seq also revealed oscillating expression of 16 long intergenic noncoding RNAs and key histone modifying enzymes critical for circadian gene expression. Our phenotypic and genotypic characterization reveals a complex global landscape of overlapping and temporally controlled networks driving the essential circadian process in the eye.—Mustafi, D., Kevany, B. M., Genoud, C., Bai, X., Palczewski, K. Photoreceptor phagocytosis is mediated by phosphoinositide signaling. *FASEB J.* 27, 4585–4595 (2013). www.fasebj.org**

Key Words: lincRNA · retina · RNA-Seq · RPE

Multiple mechanisms regulated by the circadian clock provide the selective advantage to appropriately regulate metabolism and physiology in a time-dependent manner (1). Although thousands of transcripts have exhibited circadian oscillations in peripheral tissues in the body (2), <10% of these are identical between the central suprachiasmatic nuclei (SCN) pacemaker and peripheral tissues (3). This observation emphasizes that the circadian clock network contributes to physiological responses by affecting cell-specific transcripts (4). In contrast to many other peripheral tissues, the light-sensitive retina is a unique peripheral circadian oscillator (5, 6) because it directly influences the circadian rhythms generated by the SCN through light entrainment (7, 8). The lack of significant changes in temporal disc shedding after SCN destruction (9) implicates the retina as a driver of this circadian homeostatic process. As a peripheral oscillator, the retina regulates circadian processes such as the renewal of the photoreceptor outer segments (POSs), with a peak in activity shortly after light onset in the morning and a trough later in the afternoon (10). This daily process, in which ~10% of the photoreceptor volume is shed into the subretinal space, relies on the neighboring retinal pigmented epithelium (RPE). The RPE engulfs and phagocytoses these light-sensitive portions of POSs containing not only native membranes and proteins but also toxic photooxidative products (11) for lifelong maintenance of these postmitotic neurons. Genetic defects in critical components of this

Abbreviations: B6, C57BL/6J; DAG, diacylglycerol; DAPI, 4,6-diamidino-2-phenylindole; DGKI, diacylglycerol kinase ι; HAT, histone acetyltransferase; HDAC, histone deacetylase; HMT, histone methyltransferase; IHC, immunohistochemistry; IP_3, inositol triphosphate; ITPR1, inositol 1,4,5-triphosphate receptor type 1; LAMP, lysosomal-associated membrane protein; lincRNA, long intergenic noncoding RNA; MARCKSL1, myristoylated alanine-rich C kinase substrate related protein; MerTK, Mer tyrosine kinase; mAb, monoclonal antibody; PAI-1, plasminogen activator inhibitor-1; PI3K, phosphoinositide 3-kinase; PLC, phospholipase C; pAB, polyclonal antibody; PIP_2, phosphatidylinositol-4,5-*bis*phosphate; POS, photoreceptor outer segment; RNA-Seq, RNA sequencing; RORA1, retinoid-related orphan receptor A1; RORE, retinoic acid-related orphan receptor response element; RPE, retinal pigmented epithelium; RPKM, reads per kilobase per million reads; RT-PCR, real-time-polymerase chain reaction; SBF-SEM, serial block face-scanning electron microscopy; SCN, suprachiasmatic nuclei

[1] Correspondence: Department of Pharmacology, School of Medicine, Case Western Reserve University, 10900 Euclid Ave., Cleveland, OH 44106-4965, USA. E-mail: kxp65@case.edu

doi: 10.1096/fj.13-237537

important RPE-mediated process, such as the Mer tyrosine kinase (MerTK), can lead to severe retinal degenerative phenotypes (12, 13).

Considering their role in daily phagocytosis of shed discs from ~40–60 photoreceptor cells, postmitotic RPE cells can be considered as some of the most active phagocytic cells in the body. Although much of our knowledge regarding RPE-mediated phagocytosis has been guided by the mechanism employed by professional macrophages (14), the specific steps involved in RPE-mediated phagocytosis are still poorly defined (15–17). Defining the genetic mechanisms that comprise the circadian clock is central to understanding how genomic rhythms are transformed into metabolic physiology in the eye. The molecular basis of the circadian clock has been based on interlocked transcriptional and translational feedback loops (18). Most notably, different chromatin modifications (19) that coordinate circadian regulation (20) with rhythmic histone modifications have been shown to be associated with cyclic transcription of several circadian genes (21, 22). Furthermore, histone methyltransferases are critical determinants of circadian expression of noncoding RNAs (23) that display circadian rhythm regulation as demonstrated in the closely related pineal gland (24).

To connect a phenotype to the underlying genetic drivers of circadian processes, it is essential to elucidate the phenotypic features and combine that with temporal genetic information (25). In this study, we first characterized the time-dependent phenotypic burst and trough of photoreceptor shedding and phagocytosis by serial sectioning microscopy in the murine eye. Then, transcriptional readouts were assessed on a genomic level by RNA squencing (RNA-Seq; ref. 26) to measure temporal transcript expression in the eye. This combined approach identified differentially expressed protein coding and long intergenic noncoding RNA (lincRNA) transcripts linked to the phenotypic changes related to phagocytosis in the eye.

MATERIALS AND METHODS

Animals

C57BL/6J (B6) mice were obtained from The Jackson Laboratory (Bar Harbor, ME, USA). Mice were housed in the animal facility at the School of Medicine, Case Western Reserve University (CWRU; Cleveland, OH, USA), where they were maintained on a standard chow diet in a 12 h light (~10 lux)/12 h dark cycle. All animal procedures and experiments were performed in accordance with U.S. animal protection laws and were approved by the CWRU Animal Care Committees and conformed to both the recommendations of the American Veterinary Medical Association Panel on Euthanasia and the Association of Research for Vision and Ophthalmology.

Library preparation for RNA-Seq

Mice were euthanized by cervical dislocation, and eyes were enucleated and immediately placed in RNAlater stabilization reagent (Qiagen, Valencia, CA, USA). Each eye was promptly homogenized and passed through a QIAShredder column (Qiagen) as per manufacturer's directions to further homogenize the tissue. Total RNA was then purified by using the RNeasy Mini Kit with on-column DNase treatment (Qiagen) as per manufacturer's directions. Poly(A) RNA was isolated with the Oligotex kit (Qiagen) by also following the manufacturer's instructions. Pooled total RNA samples from 5 eyes were used for each whole-eye library preparation. Three separate libraries were made for B6 mice at each of the 2 time points (1.5 and 9.0 h after lights were turned on). Library preparation for Illumina RNA-Seq (Illumina Inc., San Diego, CA, USA) was carried out as described previously (27, 28).

RNA-Seq runs, read mapping, and determination of reads per kilobase per million reads (RPKM)

Each murine eye library was run on one lane of the Genome Analyzer IIx (Illumina) in the Genomics Core Facility at CWRU by using 49- or 79-bp single-end sequencing. Data were processed and aligned with the University of California–Santa Cruz (UCSC; Santa Cruz, CA, USA) mouse genome assembly and transcript annotation (mm9) using Genomic Short-read Nucleotide Alignment Program (GSNAP), manual extraction of uniquely-mapped reads, HTseq for raw read counts of genes, and manual calculation of RPKM statistics by gene. The processed and raw fastq files were deposited at the U.S. National Center for Biotechnology Information (NCBI; Bethesda, MD, USA) Gene Expression Omnibus (GEO) database (accession no. GSE48974; http://www.ncbi.nlm.nih.gov/geo/).

Pathway generation and analysis

RNA-Seq data were analyzed with Ingenuity Pathway Analysis software (Ingenuity Systems, Redwood, CA, USA). Average RPKM values from biological replicate RNA-Seq runs at the two time points were uploaded along with gene identifiers and statistical *P* value calculations. Core analysis of a set of 12,583 mapped genes was done to identify perturbed molecular networks. Networks were generated from information contained in the Ingenuity Pathway Knowledge Base. Genes or gene families, represented as nodes, were connected to other genes by edges, supported by ≥1 reference from the literature or canonical information derived from the Ingenuity Pathway Knowledge Base. Pathway generation of differentially expressed genes was also done by hand using Ingenuity, the NCBI PubMed database (http://www.ncbi.nlm.nih.gov/pubmed/), and known retinal localization as guides.

Promoter analysis

The 5-kb promoter sequences of selected genes were searched with FIMO (29) for the CLOCK:BMAL1 and retinoid-related orphan receptor A1 (RORA1) motifs, and only those that returned significant *P* values using position-specific scoring matrix for each of the motifs in the promoter sequences were considered.

Real-time-polymerase chain reaction (RT-PCR)

Isolated total retinal RNA (2 μg) from 2 pooled B6 samples at time points 07:30 (1.5 h after lights turn on), 12:00 (6.0 h after lights turn on), and 15:00 (9.0 h after lights turn on) was converted to cDNA with the High Capacity RNA-to-cDNA kit (Applied Biosystems, Foster City, CA, USA). RT-PCR was done with TaqMan chemistry and Assays on Demand probes

(Applied Biosystems) for mouse *Bmal1* (Mm00500226_m1), *Dgki* (Mm01159464_m1), *Egr1* (Mm00656724_m1), *Marcksl1* (Mm00456784_m1), *Mertk* (Mm00434920_m1), *Npas2* (Mm00500848_m1), *PAI-1* (Mm00435860_m1), *Rasgrp3* (Mm01223826_m1), and *Rev-erbα* (Mm00520708_m1). The 18S rRNA (4319413E) probe set (Applied BioSystems) was used as the endogenous control. All real-time experiments were done in triplicate with an ABI Step-One Plus qRT-PCR machine (Applied Biosystems). Fold changes were calculated based on differences in threshold cycles (C_t) after normalization to 18S rRNA. For semiquantitative RT-PCR, 25 ng of total RNA was used in each 12.5-μl reaction as per the manufacturer's directions. Primers for the lincRNA were custom designed. Actin primers were designed for loading controls.

Serial block face-scanning electron microscopy (SBF-SEM), data analyses, and 3-dimensional reconstruction

Blocks for SBF-SEM were prepared as before (27). The prepared sample was fixed on the microtome (3View; Gatan, Pleasanton, CA, USA) attached on the door of the SEM (Quanta 200 FEG ESEM; FEI, Hillsboro, OR, USA). Cutting was initiated in the evacuated specimen chamber. To perform serial cutting of the block face, a 100-nm slice was cut from the face with a diamond knife, and the freshly cut surface of the block was imaged from the backscattered electron signal. This process was repeated sequentially in an automatic computer-controlled fashion to collect 300 successive images over ~12 h. Imaging was performed at an accelerating voltage of 3 kV in a low vacuum mode (0.23 Torr) with a scanning frame of 4096 × 4096 at a rate of 3 μs/pixel.

After serial sectioning, images were opened with Fiji-win32 (30) and merged to form a stack. The stack was registered and aligned to account for any drift that may have occurred over the time course of sectioning. The registered stack then was opened with the Reconstruct program (31), and structural elements were mapped to provide 3-dimensional reconstructions.

Histology and immunohistochemistry

Histological and immunohistochemical procedures were carried out as described previously (32). Alexa 4,6-diamidino-2-phenylindole (DAPI) and Alexa 488-conjugated peanut agglutinin (PNA) were purchased from Invitrogen (Carlsbad, CA, USA). Mouse anti-Rasgrp3 monoclonal antibody (mAb), rabbit anti-HDAC3-polyclonal antibody (pAB), rabbit anti-Clock pAb, rabbit anti-PAI-1 pAb, and mouse anti-Rev-erbα mAb were purchased from Santa Cruz Biotechnology (Santa Cruz, CA, USA), and mouse anti-β-actin monoclonal antibody was purchased from Sigma (St. Louis, MO, USA). Cy3-conjugated goat anti-mouse IgG or goat anti-rabbit IgG (Promega, Madison, WI, USA) was used as secondary antibody. Immunohistochemistry (IHC) sections were viewed with a Zeiss LSM 510 inverted laser scan confocal microscope (Carl Zeiss, Oberkochen, Germany).

Immunoblotting

Whole mouse eyes from 2 mice at each time point were homogenized in ice-cold RIPA buffer (50 mM Tris, pH 8.0; 150 mM NaCl; 1 mM EDTA; 1 mM EGTA; 1.0% Nonidet P-40; and 1% sodium deoxycholate) plus 1× protease inhibitors (Roche, San Francisco, CA, USA). A total of 100 ng of protein was loaded in each lane of a 10% SDS-PAGE gel for protein separation. Immunoblotting (Immobilon-P polyvinylidenedifluoride; Millipore, Billerica, MA, USA) was carried out according to standard protocols. Primary antibodies identical to those used for IHC were detected by incubation with horseradish peroxidase-conjugated secondary antibodies (Jackson ImmunoResearch) and visualized with SuperSignal West Pico Chemiluminescent Substrate (Thermo Scientific, Waltham, MA, USA). Anti-β-actin (AC-15; Abcam, Cambridge, MA, USA) was employed for the loading control.

RESULTS

SBF imaging highlights the circadian phenotypic variation in photoreceptor phagocytosis in the mouse eye

A peak of photoreceptor phagocytosis has been noted in mammals ~1.5 h after lights turn on in the morning, with a trough in this process noted at 9.0 h after lights turn on (10). We used SBF-SEM (27, 33) to accurately document these events across large portions of the retina by examining fixed embedded mouse eye cups from B6 mice maintained on a 12/12-h light-dark cycle at 1.5 and 9.0 h after lights were turned on. Images were taken in series through retinal tissue by scanning the block face, removing 100 nm of tissue, and scanning the freshly cut surface serially, allowing for 3-dimensional reconstructions of volumetric blocks 12 μm deep and 50 μm wide at each time point to capture photoreceptor turnover across multiple RPE cells and hundreds of photoreceptor cells (**Fig. 1**). The resulting 3-dimensional reconstructions revealed a 2.8-fold increase in phagosomal events in the RPE at the 1.5 h (Fig. 1*A*, *B*) compared with the 9.0 h (Fig. 1*C*, *D*) time point (**Table 1**), consistent with previous counts found using light microscopy of single static sections of the rat retina (10). These studies confirmed the phenotypic difference in photoreceptor phagocytosis at these time points and prompted temporal whole transcriptome RNA-Seq studies to reveal the underlying genetic architecture driving this circadian process.

Temporal RNA-Seq transcriptome analysis of the mouse eye reveals differentially expressed coding and noncoding transcripts

Three biological replicates of ocular tissues at 1.5 and 9.0 h were prepared and analyzed by RNA-Seq. Replicate results from each time point had high correlation coefficients when plotted against each other (r^2>0.92). RNA expression levels were quantified by calculating coverage in RPKM across the exons to generate sums for each transcript. The reads not only reflected transcriptional activity but also post-transcriptional processing events. Using an expression cutoff of 1 RPKM, equivalent to one transcript per cell (34), we identified a total of 13,296 protein-coding genes expressed in the whole eye between the two time points (1.5 and 9.0 h). Then, a set of 365 oscillating transcripts (2.7% of expressed) was identified with at least a 1.5-fold average differential expression between 1.5 and 9 h ($P \leq 0.05$; **Table 2**). A large cohort of oscillating protein-coding transcripts were found to be well characterized circa-

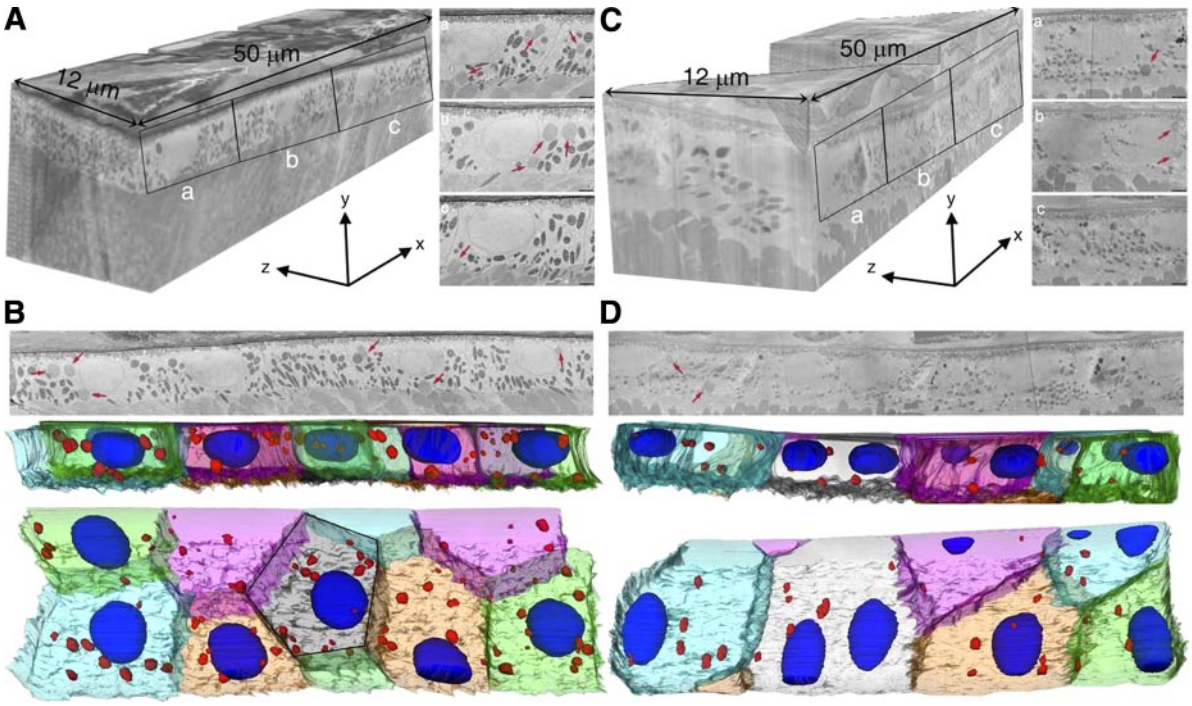

Figure 1. Visualization and quantification of circadian variation in photoreceptor phagocytosis events by SBF-SEM. *A*) B6 mouse eye sample at 1.5 h was analyzed by SBF-SEM at 100-nm serial sections and reconstruction of a volumetric block of retina 12 μm deep and 50 μm wide, allowing capture of multiple RPE cells at sufficient depth. *a–c*) Views across 3 fields of view that were taken at high resolution and stitched together for data analysis. Red arrows in *a–c* show phagocytosis events in RPE cells. *B*) SEM image of the RPE cell layer, with the resulting 3-dimensional reconstructions below in plane and tangential to reveal phagosomal events (denoted in red) throughout the RPE cell layer. The central cell exhibits the characteristic hexagonal RPE cell morphology. Given the surface area and rod density, there was an observed 14% rate of phagocytosis events. *C*) Similarly, SBF-SEM of a B6 mouse eye sample at 9.0 h was processed as described in *A*. *a–c*) Views across 3 fields of view that were taken at high resolution and stitched together for data analysis. Red arrows in the panels, less numerous than in *A*, highlight phagocytosis events in RPE cells. *D*) SEM image of the RPE cell layer at 9.0 h along with the resulting 3-dimensional reconstructions shown below were obtained as described in *B*. Phagosomal events denoted in red throughout the RPE cell layer are less than seen in *B*, but double nucleated RPE cells are visible in this view. Given the surface area and rod density, there was an observed 5% rate of phagocytosis events, a 2.8-fold attenuation from the morning time point ($P<0.0001$). Scale bars = 1 μm.

dian clock genes and their downstream effectors, such as *Bmal1*, *Clock*, *Dbp*, *Egr1*, *Fos*, *Npas2*, *Nr1d1* (*Rev-erbα*), and *Rorc* (**Fig. 2*A*** and ref. 35). The expression differences identified between the time points by RNA-Seq were in good agreement with the differences assessed by RT-PCR of selected targets (**Table 3**). However, transcript oscillations were not limited to protein-coding loci. Of the 191 detected lincRNAs at the two time points, 16 displayed oscillating expression (Fig. 2*B*). Ensembl lincRNA transcript ENSMUST0000013486 displayed the most robust differential expression, with a 9.8-fold enrichment at 9.0 h compared with 1.5 h. With pathway analysis of these differential expressed transcripts implicating circadian rhythm signaling as the most overrepresented biological process, we then sought to identify those transcripts that may be involved in photoreceptor phagocytosis.

Temporal cycling of core clock network genes in the eye and their localization in RPE cells

The circadian clock has transcriptional/translational feedback loops that regulate its rhythmic expression and activity. The positive limb consists of *Bmal1, Clock, and Npas2*, and the negative limb consists of the period and cryptochrome genes (36, 37). The positive limb is rein-

TABLE 1. *Temporal SBF-SEM imaging reveals differences in photoreceptor phagocytosis events in the RPE of B6 mice*

	Time point	
Parameter	1.5 h	9.0 h
RPE cells imaged	8	6
Phagosomal events/cell slice imaged	0.14 ± 0.02	0.05 ± 0.02

SBF-SEM carried out as described in Materials and Methods.

TABLE 2. *Temporal RNA-Seq expression profile of the B6 mouse eye*

Parameter	Protein-coding genes	lincRNAs
Total transcripts (≥1 RPKM)	13,296	191
Differentially expressed transcripts	365 (3%)	16 (8%)
Fold difference >2.00	78	12
Fold difference 1.75–2.00	78	1
Fold difference 1.60–1.75	86	2
Fold difference 1.50–1.60	123	1

Transcripts identified by RNA-Seq at the 1.5 *vs.* 9.0 h time points.

forced by activating RORs whereas Rev-erbα/β (*Nr1d1/2*) function as transcriptional repressors to reinforce the negative limb (38–40). Our temporal RNA-Seq data revealed that elements of the positive limb were more highly expressed at 1.5 h, whereas elements of the negative limb were more highly expressed at 9.0 h (**Fig. 3*A***). Given that the master controller in circadian signaling *Clock* possess critically important histone acetyltransferase (HAT) activity (41), we examined the differential expression profile of histone modifying enzymes (19). This analysis revealed that only histone methyltransferases (HMTs), *Mll1*, *Mll3*, and *Ash1l*, all of which act on histone H3 at Lys4, displayed oscillating expression with en-

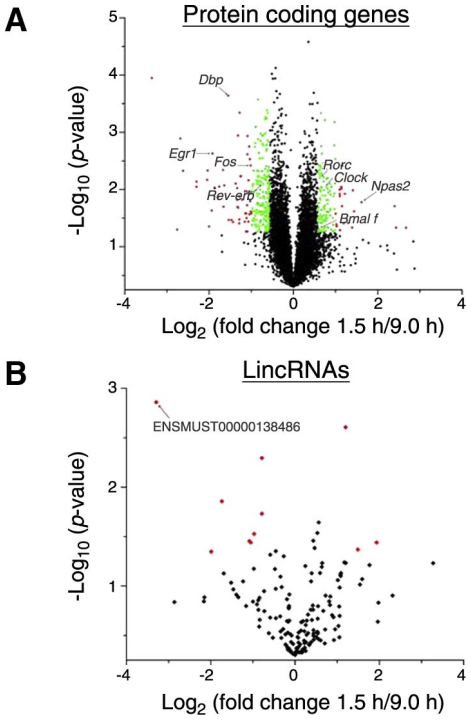

Figure 2. Temporal oscillation of the coding and noncoding RNA transcripts in B6 mouse eyes revealed by RNA-Seq. Volcano plot comparisons of transcript expression between 1.5 and 9.0 h time points in the mouse eye. *A*) Examination of protein coding gene expression ($\log_2$ scale) across 3 biological replicates for each time point plotted against the statistical significance of the difference in expression (*P* value in a $\log_{10}$ scale) reveals that most transcripts do not show significant changes in expression (black points), whereas those that evidenced a 1.5–2.0 fold change in expression are represented by green points, and those with >2.0 fold change in expression are displayed as red points. Key circadian clock genes are labeled. *B*) Examination of long intergenic noncoding gene expression ($\log_2$ scale) across 3 biological replicates for each time point plotted *vs.* the statistical significance of the difference in expression (*P* value in a $\log_{10}$ scale) reveals the oscillating transcripts pictured as red points, with the most differentially expressed lincRNA transcript labeled.

TABLE 3. *RT-PCR verification of differential expression*

Gene	Fold difference	
	RNA-Seq	RT-PCR
Bmal1	1.5	2.0 ± 0.1
Dgki	1.9	1.5 ± 0.1
Egr1	−3.8	−3.4 ± 0.7
Marcksl1	−2.1	−1.7 ± 0.3
Mertk	1.0	1.0 ± 0.1
Npas2	3.1	2.3 ± 0.5
Nr1d1 (Rev-erb α)	−1.7	−1.6 ± 0.1
Rasgrp3	1.5	1.5 ± 0.2
Serpine1	−2.4	−1.8 ± 0.2

Transcripts identified by RNA-Seq at the 1.5 *vs.* 9.0 h time points.

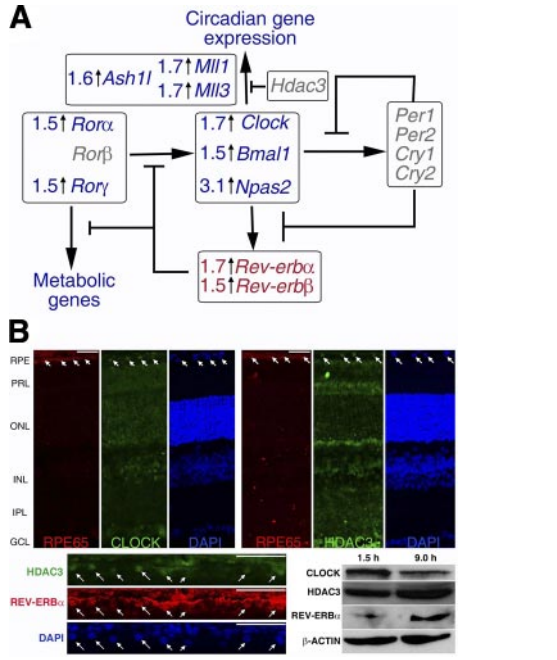

Figure 3. Oscillations in core circadian signaling components and their localization to the RPE layer in the mouse eye. *A*) Examination of temporal gene expression (fold change denoted in red if higher at 1.5 h, fold change denoted in blue if higher at 9.0 h, with no change denoted in gray) highlights the differential expression of positive and negative limb circadian clock genes along with histone methyltransferases. *B*) IHC staining of mouse eye cups for CLOCK, HDAC3, and REV-ERBα revealed that these proteins are located in the RPE cells, most notably in the nucleus as the signals from these circadian proteins overlap with the nuclear DAPI stain but not the cytosolic RPE65 signal (denoted by white arrows). Immunoblots for protein level expression also mirror the fold changes seen at the transcript level between 1.5 and 9.0 h. Scale bars = 20 μm.

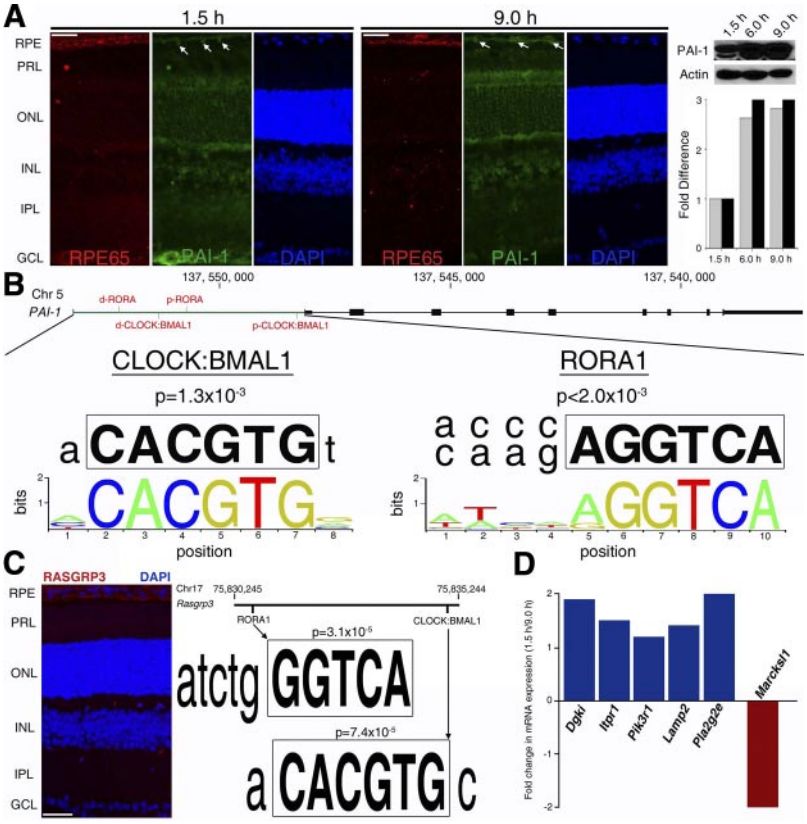

Figure 4. Identification of oscillating networks implicated in regulating RPE-mediated photoreceptor phagocytosis. *A*) PAI-1, a protein product implicated in regulation of photoreceptor phagocytosis, was found more highly expressed in the RPE of B6 mice by IHC staining at 9.0 h as compared with 1.5 h. Immunoblots of protein expression at 1.5, 6.0, and 9.0 h revealed a robust induction hours after phagocytosis, quantified at bottom (black bars), which mirrors the transcript level changes by RT-PCR (gray bars). *B*) Examination of the 5-kb promoter region of *PAI-1* revealed distal (d) and proximal (p) sites for CLOCK:BMAL1 and RORA1 motifs, with *P* values indicated for the motif occurrence from the positional scoring matrix shown. *C*) Phosphoinositide signaling genes also display robust differential expression, with RasGRP3 localizing to the RPE compartment in B6 mouse eyes with *P* values for expression of CLOCK:BMAL1 and RORA1 promoter motifs in the 5-kb promoter region. *D*) Moreover, genes involved in positive regulation (blue bars) of phosphoinositide-mediated phagocytosis such as *Dgki, Itpr1, Pik3r1, Lamp2*, and *Pla2g2e* were enriched in expression at 1.5 h, whereas those participating in negative regulation (red bar), such as *Marcksl1*, were enriched in expression at 9.0 h. Scale bars = 20 μm.

hanced expression at 1.5 h. Expression of histone deacetylases (HDACs), such as HDAC3, were unchanged temporally (Fig. 3*A*).

Elements of the circadian clock have been localized to the mammalian retina (42, 43), but we sought to ascertain whether these proteins were expressed in the RPE cell layer, and thus could modulate cellular physiology associated with photoreceptor phagocytosis. IHC staining of B6 mouse eye cups revealed that different elements of the circadian pathway, CLOCK, HDAC3, and REV-ERBα, all localized to the nuclei of RPE cells, as their signals overlapped with the nuclear DAPI stain but not the cytoplasmic signal of RPE65 (Fig. 3*B*). Moreover, the protein levels of these circadian clock elements in the eye at 1.5 and 9.0 h strongly correlated with transcript abundances obtained by RNA-Seq (Fig. 3*B*). The differential expression of these interconnecting circadian gene networks in the eye and localization to the RPE cell layer prompted us to investigate those effector transcripts that could temporally modulate photoreceptor phagocytosis.

Genetic elements that drive or inhibit photoreceptor phagocytosis are temporally segregated

One of the genes that displayed robust differential expression between 1.5 and 9.0 h was plasminogen activator inhibitor-1 (PAI-1; also known as SERPINE1), a gene previously implicated in modulating photoreceptor outer segment uptake (44) and shown to be produced by human RPE (45). Examination of B6 mouse eye cups by IHC revealed a greater PAI-1 signal in the RPE cell layer at 9.0 h compared with 1.5 h, consistent with RNA-Seq data. Also, protein levels of PAI-1 very strongly mirrored the transcript expression assessed by RT-PCR at different time points in the eye (**Fig. 4*A***). As the promoter of the human *PAI-1* revealed elements for CLOCK:BMAL1 (46, 47) and REV-ERBα (48) mediating circadian expression modulation, we examined the 5-kb promoter region of mouse *PAI-1* and similarly found proximal and distal E-box and retinoic acid-related orphan receptor response elements (ROREs) for binding of CLOCK:BMAL1 and REV-ERBα, respectively (Fig. 4*B*).

Further analysis of the differential expression profile revealed not only an enrichment in genes involved in polyphosphoinositide metabolism but also that a set of these genes was cooccupied by *Rev-erbα/β* and *Bmal1* from circadian cistromic studies of the liver (49). One of these genes, *Rasgrp3*, which has been implicated in polyphosphoinositide-signaling-directed phagocytosis (50), is expressed 1.5-fold higher at 1.5 h compared with 9.0 h, preferentially localizes in the RPE/choroid area of the B6 murine eye, and contains promoter binding motifs in the 5-kb promoter region for CLOCK:BMAL1 and REV-ERBα (Fig. 4*B*). Examination of this gene network also revealed an enrichment of those genes involved in the polyphosphoinositide metabolism and associated phagocytosis processing at 1.5 h (51), whereas there was enrichment at 9 h for those genes that would serve to sequester and limit polyphosphoinositide metabolism and thus inhibit phagocytosis (ref. 52 and Fig. 4*D*). Moreover, a cohort of these genes

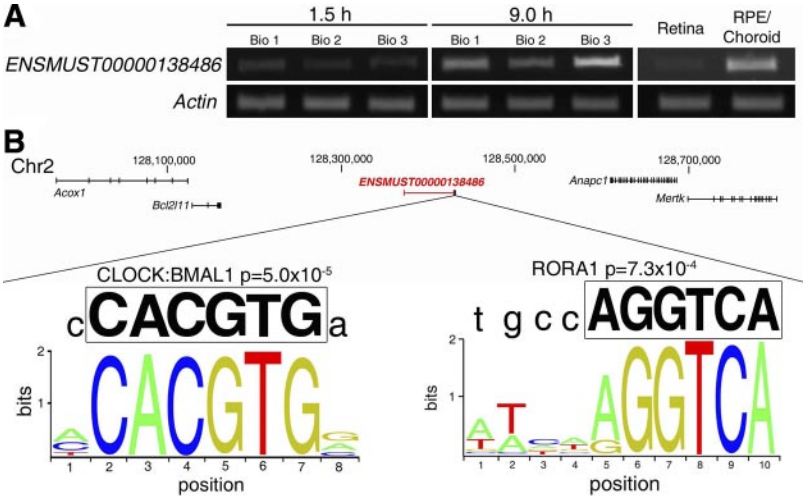

Figure 5. Location in the mouse genome and promoter motif analysis of an oscillating lincRNA controlled by circadian regulation. *A*) *ENSMUST00000138486* was found by RNA-Seq to be the most differentially expressed lincRNA transcript between 1.5 and 9.0 h, an observation verified by RT-PCR from 3 biological replicates. Examination of B6 mice revealed that this lincRNA is more highly expressed in the RPE/choroid than the retina. *Actin* was used for a loading control. *B*) Examination of genomic loci revealed that the lincRNA lies near the *Mertk* locus, an essential gene involved in photoreceptor phagocytosis. The 5-kb promoter region relative to the transcribed region of this lincRNA revealed sequences for CLOCK:BMAL1 and RORA1 promoter motifs. Associated *P* values for sequence occurrence from the positional scoring matrix are shown.

have been shown to be preferentially expressed in the retina and RPE compartments (53–55) and associate with critical RPE receptors mediating phagocytosis such as MerTK (56). Photoreceptor phagocytosis modulation may not be confined to protein coding genes. The robust differential expression of lincRNA transcript *ENMUST00000138486* was confirmed by RT-PCR, and its expression was shown to be greatly enriched in the RPE/choroid compared with the retina in B6 mice (**Fig. 5*A***). Moreover, examination of the genomic locus of this lincRNA in mice revealed that it is located near *Mertk*, with a 5-kb promoter region containing promoter motifs for binding of CLOCK:BMAL1 and REV-ERBα (Fig. 5*B*).

DISCUSSION

In more complex organisms, circadian clocks are essential for maintaining metabolic homeostasis, but the question remains how this machinery coordinates cell-specific metabolism. The prevailing idea is that circadian clocks control cellular physiology through transcription as anywhere from 3 to 20% of transcripts in various mouse tissues undergo circadian oscillations (57). High-throughput RNA-Seq offers a global approach to reveal rhythmic mRNA and noncoding RNA expression (58) that function in a specific tissue or cell type (59). In the retina, which acts as a peripheral oscillator, the circadian process of photoreceptor disc shedding and RPE-mediated phagocytosis (9, 11) is essential for renewal of postmitotic photoreceptors.

First, we established specific time points for RNA-Seq to connect the genotypic features to the phenotypic variation in the murine eye using SBF-SEM (Fig. 1). Temporal RNA-Seq studies at the peak and trough of photoreceptor phagocytosis revealed that 3% of coding and 8% of lincRNA transcripts undergo oscillating expression (Fig. 2). The core clock genes displayed robust oscillations as did key histone modifying enzymes (Fig. 3), which could temporally modulate key downstream effector genes. Further examination revealed key genes and networks centered on lipid signaling pathways that localize to the RPE layer and contain promoter elements that explain their role as effector clock output genes potentially driving photoreceptor phagocytosis (Fig. 4).

Photoreceptor disc shedding and RPE-mediated phagocytosis are mediated by a complex sequence of steps by both the photoreceptor and RPE layers. It begins with shedding of photoreceptor outer segment discs, which expose phosphotidylserine at the tips of photoreceptors in a circadian matter (60) to facilitate binding to $\alpha_v\beta_5$ (61) and CD36 (62) receptors on the apical surface of RPE cells. Our data revealed rhythmic expression of a gene that can directly modulate this step. The serine protease inhibitor *PAI-1* displayed higher expression at 9.0 h compared with 1.5 h after lights were turned on, which was also reflected at the protein level and by IHC staining of the B6 mouse eye photoreceptor and RPE cell layers (Fig. 4*A*). PAI-1 has previously been shown to decrease binding of shed discs to RPE cells (44), which is thought to be mediated by regulation of the interaction of vitronectin with an integrin receptor (63) and can explain the loss in synchronized retinal phagocytosis in mice lacking the vitronectin $\alpha_5\beta_5$-integrin receptor (64). The role of PAI-1 in reducing phagocytotic activity is not limited to RPE cells as it has also been demonstrated in microglial cells (65). Moreover, PAI-1 acts as important "don't eat me" signal for viable cells as its deficiency leads to increased phagocytosis by neutrophils (66). Temporal variation of *PAI-1* expression could result from differential binding of circadian transcription factors in the eye. Examination of the 5-kb promoter region of mouse *PAI-1* revealed E-box and RORE motifs for binding of CLOCK:BMAL1 and REV-ERBα, respectively (Fig. 4*B*). It has been shown that increased *Bmal1* expression precedes peak PAI-1 mRNA expression by 6 to 12 h (46, 47), whereas REV-ERBα then represses PAI-1 gene expression (48), consistent with our RNA-Seq readouts for the expression profile of these genes.

Furthermore, we found that circadian mechanisms controlling phagocytosis are not confined to the step of disc binding but are also associated with the internalization and further downstream steps mediated by MerTK (12, 67). RPE cells challenged with shed discs phosphorylate MerTK (68), forming a functional docking site for phospholipase C (PLC) phosphorylation and activation (69). PLC can then hydrolyze phosphatidylinositol-4,5-*bis*phosphate (PIP_2), present in large quantities in the inner leaflet of the plasma membrane, to the second messengers diacylglycerol (DAG) and inositol triphosphate (IP_3), causing increases in free Ca^{2+} levels. Lipid modification by receptor signaling can radiate signals and affect large areas of the plasma membrane, and phosphoinositide metabolism has been shown to play an essential role in phagocytosis. However, PIP_2 metabolism in the forming phagosome is localized (70), highlighting how this process is confined to only those areas of the retina in which 10% of the photoreceptors are shedding their discs.

Our data reveal differentially expressed genes at each step of this lipid signaling pathway (Fig. 4*C*, *D*), with a peak in expression at 1.5 h of genes driving this process coinciding with the burst of photoreceptor phagocytosis. Increased expression of inositol 1,4,5-triphosphate receptor type 1 (*Itpr1*) at 1.5 h, shown to be important for the internalization phase of phagocytosis (71), can drive increases in Ca^{2+} levels from internal endoplasmic reticulum stores (72). The second phosphoinositide metabolite, DAG, not only accumulates at the forming phagocytic cup (73) but also recruits effector proteins with conserved protein kinase C type I (C1) domains (74). In this manner, we see that DAG can recruit those effectors that display elevated expression at 1.5 h, such as RasGRPs containing the C1 domain (75), to the phagosome. Once relocated, RasGRP3 can drive further phagocytosis signaling (50), whereas diacylglycerol kinase ι (Dgki), which is also increased at 1.5 h and restricted in expression to the brain and retina (53), can associate with RasGRP3 and metabolize DAG (76) to limit RasGRP3 function. Ultimately, maturation of the phagosome leads to recruitment of the

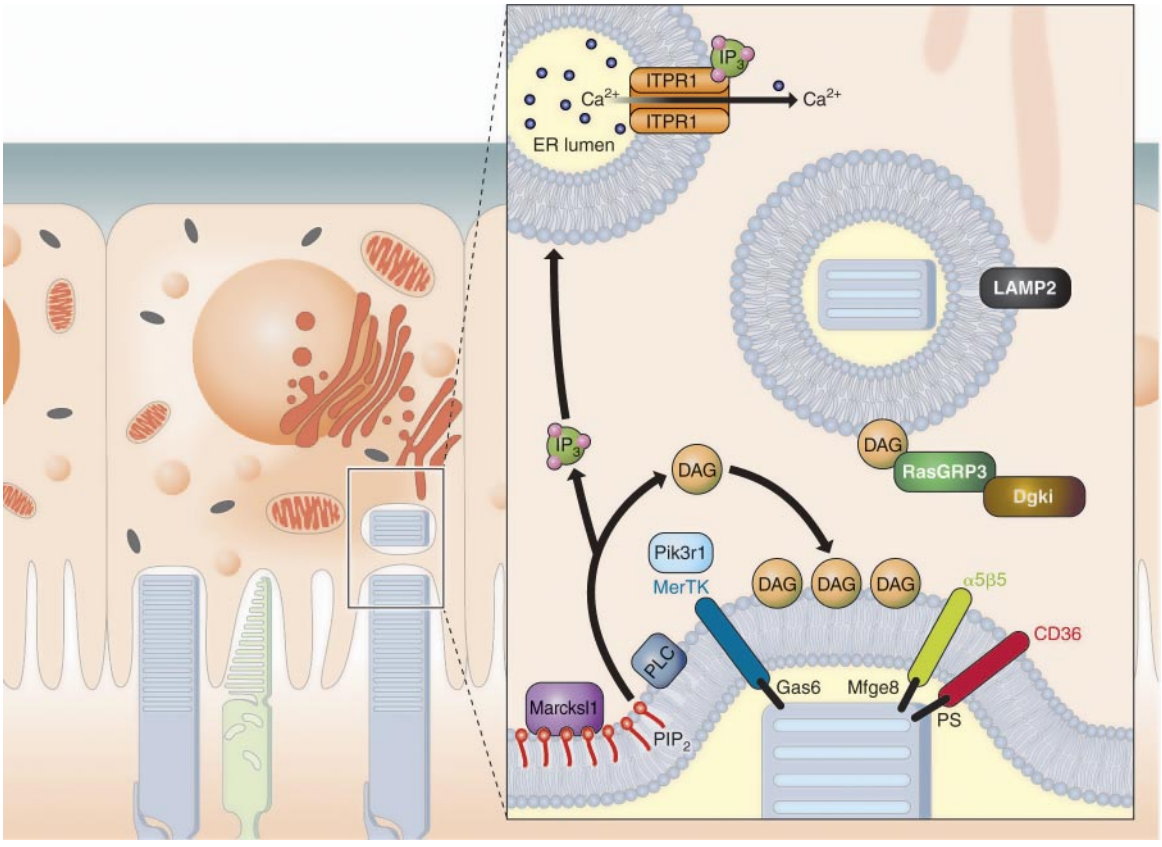

Figure 6. Phosphoinositide lipid signaling as a central player in RPE-mediated photoreceptor phagocytosis. Photoreceptor discs shed in a circadian rhythm into the subretinal space are phagocytosed by the neighboring RPE for processing. These data implicated circadian cycling of key elements involved in phosphoinositide lipid signaling as drivers of this process. RPE ingestion, which is centered on the MerTK receptor, can activate the function of PLC and facilitate the turnover of PIP_2 into the effector molecules IP_3 and DAG. This lipid metabolism is required to mediate the downstream steps as DAG accumulates at the phagocytic cup to facilitate ingestion and to recruit C1 domain containing proteins such as RasGRP3 to ingest disc membranes for further processing as they transition to lysosomal breakdown facilitated by proteins such as LAMP2. IP_3 can bind to IP_3-mediated calcium channels such as ITPR1 and thereby release Ca^{2+}, which is also important for the internalization phase. Closure of phagocytic cups is mediated by PI3-kinases, one of which, Pik3r1, directly binds to MerTK. Finally, mechanisms exist to blunt this process by sequestering PIP_2 availability by lateral domains of proteins such as Marcksl1, which shows peak expression that coincides with the trough in photoreceptor phagocytosis.

lysosomal-associated membrane proteins (LAMPs; ref. 77). Thus, we observed increased expression of *Lamp2*, a gene previously shown to be enriched in the RPE of the eye (55). The final step of this process involves closure of the phagocytic membrane by phosphoinositide 3-kinase (PI3K; ref. 78). Here we found increased expression of only 1 PI3K, the regulatory subunit *Pik3r1*, which not only has been shown to localize to RPE cells but also to interact with MerTK, the key receptor involved in internalization and downstream signaling (56). In contrast, at the 9.0 h time point, we documented increased expression of a key gene, myristoylated alanine-rich C kinase substrate related protein (*Marcksl1*), which serves to counteract this lipid signaling pathway activated at 1.5 h. Sequestering PIP_2 markedly inhibits this cascade; therefore, it would be critical to keep this metabolite sequestered during periods when discs are not actively shed by the photoreceptors. *Marcksl1*, which regulates PIP_2 availability by its lateral domains (79) through colocalization adjacent to forming phagocytic cups (80), can be regulated by integrins (81). Therefore, oscillating transcripts in the lipid signaling network highlight the complexity that drives photoreceptor phagocytosis in a circadian manner (**Fig. 6**).

The control exerted by the circadian clock on these oscillating transcripts is verified by examining the circadian gene expression levels of REV-ERB/BMAL1 at common cistromic sites. *Rev-erbα/β* share cistromic overlap with a set of genes that are also controlled by *Bmal1* and thus cooperate to regulate clock output genes such as *Itpr1*, *Pik3r1*, and *Rasgrp3* (49), all genes implicated from our data to drive the lipid signaling pathway underlying photoreceptor phagocytosis. Moreover, binding of BMAL1 and REV-ERBα/β at numerous sites outside of well-characterized promoter elements of protein coding genes (49, 82) indicates that these sites could relate to promoters of novel noncoding transcripts such as lincRNAs that have also displayed robust circadian oscillations in peripheral tissues (83). This supposition is consistent with findings that a lincRNA resides in the mouse genome in close proximity to *Mertk* and contains E-box and RORE features to drive its circadian expression profile (Fig. 5).

The oscillating expression of lincRNA transcripts and HMTs in the eye reveals another layer of complexity that may influence photoreceptor phagocytosis. Whereas the universal function of lincRNAs has yet to be elucidated, these transcripts are thought to have a role in maintaining vision in adults (84). The cistromic landscape of the core circadian transcriptional regulators reveals that the majority of expressed genes undergo circadian histone modifications irrespective if RNA expression levels cycle (85). Given that genetic disruption of these histone-modifying elements can affect regulation of circadian gene expression and create imbalances in metabolic homeostasis (86), it will be important to understand how HMT genes *Ash1l*, *Mll1*, and *Mll3*, all of which display increased expression at 1.5 h, could be priming the RPE for the peak in phagocytosis. It has been shown that *Mll1* and *Mll3* are critical to drive circadian gene expression (22, 23) whereas *Ash1l* is associated with active genes with a pattern of occupancy closely matching that of *Mll1* (87). Mll1 and Clock operate in parallel to control the stringency of circadian gene expression (22), whereas Mll3 seems to coordinate genome-wide circadian transcription with Mll3-binding sites and shifts to intergenic regions during the course of the day, indicating its possible role in mediating circadian expression of lincRNAs (23). These findings highlight the intricacies that exist in the genomic architecture of the eye that serve to tightly control the circadian process of photoreceptor phagocytosis and maintain the health of postmitotic photoreceptors over the lifetime of the organism. Emerging technologies utilizing genome wide small interfering RNA screens in model systems can potentially reveal other members of the circadian system that may underlie cell specific processes (88). FJ

The authors thank Dr. Leslie T. Webster, Jr. [Case Western Reserve University (CWRU)] for valuable comments on the manuscript. The authors thank Neil Molyneaux, Simone Edelheit, and Milena Rajak (CWRU) for technical assistance and Dr. Ahmad Khalil (CWRU) for helpful discussions. Research reported in this work was supported by the National Eye Institute of the U.S. National Institutes of Health (NIH) under awards R01-EY-008061, R01-EY-019478, R01-EY-022606, R01-EY-022326, and P30-EY-11373, and the Research to Prevent Blindness Foundation, Foundation Fighting Blindness, Fight for Sight, and the Ohio Lions Eye Research Foundation. D.M. was supported in part by the CWRU Medical Scientist Training Program (T32GM007250) and Visual Sciences Training Program (T32EY007157) training grants from the NIH as well as the Maurice E. Müller Foundation of Switzerland. K.P. is John H. Hord Professor of Pharmacology.

REFERENCES

1. Asher, G., and Schibler, U. (2011) Crosstalk between components of circadian and metabolic cycles in mammals. *Cell Metab.* **13,** 125–137
2. Hogenesch, J. B., and Ueda, H. R. (2011) Understanding systems-level properties: timely stories from the study of clocks. *Nat. Rev. Genet.* **12,** 407–416
3. Panda, S., Antoch, M. P., Miller, B. H., Su, A. I., Schook, A. B., Straume, M., Schultz, P. G., Kay, S. A., Takahashi, J. S., and Hogenesch, J. B. (2002) Coordinated transcription of key pathways in the mouse by the circadian clock. *Cell* **109,** 307–320
4. Abruzzi, K. C., Rodriguez, J., Menet, J. S., Desrochers, J., Zadina, A., Luo, W., Tkachev, S., and Rosbash, M. (2011) Drosophila CLOCK target gene characterization: implications for circadian tissue-specific gene expression. *Genes Dev.* **25,** 2374–2386
5. Yamazaki, S., Numano, R., Abe, M., Hida, A., Takahashi, R., Ueda, M., Block, G. D., Sakaki, Y., Menaker, M., and Tei, H. (2000) Resetting central and peripheral circadian oscillators in transgenic rats. *Science* **288,** 682–685
6. Tosini, G., and Menaker, M. (1996) Circadian rhythms in cultured mammalian retina. *Science* **272,** 419–421
7. Lee, H. S., Nelms, J. L., Nguyen, M., Silver, R., and Lehman, M. N. (2003) The eye is necessary for a circadian rhythm in the suprachiasmatic nucleus. *Nat. Neurosci.* **6,** 111–112
8. Huang, W., Ramsey, K. M., Marcheva, B., and Bass, J. (2011) Circadian rhythms, sleep, and metabolism. *J. Clin. Invest.* **121,** 2133–2141
9. Terman, J. S., Reme, C. E., and Terman, M. (1993) Rod outer segment disk shedding in rats with lesions of the suprachiasmatic nucleus. *Brain Res.* **605,** 256–264

10. Lavail, M. M. (1976) Rod outer segment disk shedding in rat retina - relationship to cyclic lighting. *Science* **194,** 1071–1073
11. Kevany, B. M., and Palczewski, K. (2010) Phagocytosis of retinal rod and cone photoreceptors. *Physiology* **25,** 8–15
12. Gal, A., Li, Y., Thompson, D. A., Weir, J., Orth, U., Jacobson, S. G., Apfelstedt-Sylla, E., and Vollrath, D. (2000) Mutations in MERTK, the human orthologue of the RCS rat retinal dystrophy gene, cause retinitis pigmentosa. *Nat. Genet.* **26,** 270–271
13. D'Cruz, P. M., Yasumura, D., Weir, J., Matthes, M. T., Abderrahim, H., LaVail, M. M., and Vollrath, D. (2000) Mutation of the receptor tyrosine kinase gene Mertk in the retinal dystrophic RCS rat. *Hum. Mol. Genet.* **9,** 645–651
14. Flannagan, R. S., Cosio, G., and Grinstein, S. (2009) Antimicrobial mechanisms of phagocytes and bacterial evasion strategies. *Nat. Rev. Microbiol.* **7,** 355–366
15. Heth, C. A., and Marescalchi, P. A. (1994) Inositol triphosphate generation in cultured rat retinal-pigment epithelium. *Invest. Ophth. Vis. Sci.* **35,** 409–416
16. Heth, C. A., Marescalchi, P. A., and Ye, L. Y. (1995) Ip3 generation increases rod outer segment phagocytosis by cultured royal-college of surgeons retinal-pigment epithelium. *Invest. Ophth. Vis. Sci.* **36,** 984–989
17. Hall, M. O., Burgess, B. L., Abrams, T. A., and Martinez, M. O. (1996) Carbachol does not correct the defect in the phagocytosis of outer segments by royal college of surgeons rat retinal pigment epithelial cells. *Invest. Ophth. Vis. Sci.* **37,** 1473–1477
18. Dunlap, J. C. (1999) Molecular bases for circadian clocks. *Cell* **96,** 271–290
19. Kouzarides, T. (2007) Chromatin modifications and their function. *Cell* **128,** 693–705
20. Masri, S., and Sassone-Corsi, P. (2010) Plasticity and specificity of the circadian epigenome. *Nat. Neurosci.* **13,** 1324–1329
21. Etchegaray, J. P., Lee, C., Wade, P. A., and Reppert, S. M. (2003) Rhythmic histone acetylation underlies transcription in the mammalian circadian clock. *Nature* **421,** 177–182
22. Katada, S., and Sassone-Corsi, P. (2010) The histone methyltransferase MLL1 permits the oscillation of circadian gene expression. *Nat. Struct. Mol. Biol.* **17,** 1414–1421
23. Valekunja, U. K., Edgar, R. S., Oklejewicz, M., van der Horst, G. T., O'Neill, J. S., Tamanini, F., Turner, D. J., and Reddy, A. B. (2013) Histone methyltransferase MLL3 contributes to genome-scale circadian transcription. *Proc. Natl. Acad. Sci. U. S. A.* **110,** 1554–1559
24. Coon, S. L., Munson, P. J., Cherukuri, P. F., Sugden, D., Rath, M. F., Moller, M., Clokie, S. J., Fu, C., Olanich, M. E., Rangel, Z., Werner, T., Program, N. C. S., Mullikin, J. C., and Klein, D. C. (2012) Circadian changes in long noncoding RNAs in the pineal gland. *Proc. Natl. Acad. Sci. U. S. A.* **109,** 13319–13324
25. Lehner, B. (2013) Genotype to phenotype: lessons from model organisms for human genetics. *Nat. Rev. Genet.* **14,** 168–178
26. Wang, Z., Gerstein, M., and Snyder, M. (2009) RNA-Seq: a revolutionary tool for transcriptomics. *Nat. Rev. Genet.* **10,** 57–63
27. Mustafi, D., Kevany, B. M., Genoud, C., Okano, K., Cideciyan, A. V., Sumaroka, A., Roman, A. J., Jacobson, S. G., Engel, A., Adams, M. D., and Palczewski, K. (2011) Defective photoreceptor phagocytosis in a mouse model of enhanced S-cone syndrome causes progressive retinal degeneration. *FASEB J.* **25,** 3157–3176
28. Mustafi, D., Maeda, T., Kohno, H., Nadeau, J. H., and Palczewski, K. (2012) Inflammatory priming predisposes mice to age-related retinal degeneration. *J. Clin. Invest.* **122,** 2989–3001
29. Grant, C. E., Bailey, T. L., and Noble, W. S. (2011) FIMO: scanning for occurrences of a given motif. *Bioinformatics* **27,** 1017–1018
30. Schindelin, J., Arganda-Carreras, I., Frise, E., Kaynig, V., Longair, M., Pietzsch, T., Preibisch, S., Rueden, C., Saalfeld, S., Schmid, B., Tinevez, J. Y., White, D. J., Hartenstein, V., Eliceiri, K., Tomancak, P., and Cardona, A. (2012) Fiji: an open-source platform for biological-image analysis. *Nat. Meth.* **9,** 676–682
31. Fiala, J. C. (2005) Reconstruct: a free editor for serial section microscopy. *J. Microsc.* **218,** 52–61
32. Maeda, A., Maeda, T., Imanishi, Y., Kuksa, V., Alekseev, A., Bronson, J. D., Zhang, H. B., Zhu, L., Sun, W. Y., Saperstein, D. A., Rieke, F., Baehr, W., and Palczewski, K. (2005) Role of photoreceptor-specific retinol dehydrogenase in the retinoid cycle in vivo. *J. Biol. Chem.* **280,** 18822–18832
33. Denk, W., and Horstmann, H. (2004) Serial block-face scanning electron microscopy to reconstruct three-dimensional tissue nanostructure. *PLoS Biol.* **2,** e329
34. Mortazavi, A., Williams, B. A., McCue, K., Schaeffer, L., and Wold, B. (2008) Mapping and quantifying mammalian transcriptomes by RNA-Seq. *Nat. Meth.* **5,** 621–628
35. Feng, D., and Lazar, M. A. (2012) Clocks, metabolism, and the epigenome. *Mol. Cell* **47,** 158–167
36. Schibler, U., and Sassone-Corsi, P. (2002) A web of circadian pacemakers. *Cell* **111,** 919–922
37. Reppert, S. M., and Weaver, D. R. (2002) Coordination of circadian timing in mammals. *Nature* **418,** 935–941
38. Takeda, Y., Kang, H. S., Angers, M., and Jetten, A. M. (2011) Retinoic acid-related orphan receptor gamma directly regulates neuronal PAS domain protein 2 transcription in vivo. *Nucleic Acids Res.* **39,** 4769–4782
39. Sato, T. K., Panda, S., Miraglia, L. J., Reyes, T. M., Rudic, R. D., McNamara, P., Naik, K. A., Fitzgerald, G. A., Kay, S. A., and Hogenesch, J. B. (2004) A functional genomics strategy reveals rora as a component of the mammalian circadian clock. *Neuron* **43,** 527–537
40. Preitner, N., Damiola, F., Molina, L. L., Zakany, J., Duboule, D., Albrecht, U., and Schibler, U. (2002) The orphan nuclear receptor REV-ERB alpha controls circadian transcription within the positive limb of the mammalian circadian oscillator. *Cell* **110,** 251–260
41. Doi, M., Hirayama, J., and Sassone-Corsi, P. (2006) Circadian regulator CLOCK is a histone acetyltransferase. *Cell* **125,** 497–508
42. Liu, X., Zhang, Z., and Ribelayga, C. P. (2012) Heterogeneous expression of the core circadian clock proteins among neuronal cell types in mouse retina. *Plos One* **7,** e50602
43. Tosini, G., Davidson, A. J., Fukuhara, C., Kasamatsu, M., and Castamon-Cervantes, O. (2007) Localization of a circadian clock in mammalian photoreceptors. *FASEB J.* **21,** 3866–3871
44. Chowers, I., Kim, Y. H., Farkas, R. H., Gunatilaka, T. L., Hackam, A. S., Campochiaro, P. A., Finnemann, S. C., and Zack, D. J. (2004) Changes in retinal pigment epithelial gene expression induced by rod outer segment uptake. *Invest. Ophth. Vis. Sci.* **45,** 2098–2106
45. Moisseiev, J., Jerdan, J. A., Dyer, K., Maglione, A., and Glaser, B. M. (1990) Retinal-pigment epithelium-cells can influence endothelial-cell plasminogen activators. *Invest. Ophth. Vis. Sci.* **31,** 1070–1078
46. Maemura, K., de la Monte, S. M., Chin, M. T., Layne, M. D., Hsieh, C. M., Yet, S. F., Perrella, M. A., and Lee, M. E. (2000) CLIF, a novel cycle-like factor, regulates the circadian oscillation of plasminogen activator inhibitor-1 gene expression. *J. Biol. Chem.* **275,** 36847–36851
47. Schoenhard, J. A., Smith, L. H., Painter, C. A., Eren, M., Johnson, C. H., and Vaughan, D. E. (2003) Regulation of the PAI-1 promoter by circadian clock components: differential activation by BMAL1 and BMAL2. *J. Mol. Cell. Cardiol.* **35,** 473–481
48. Wang, J., Yin, L., and Lazar, M. A. (2006) The orphan nuclear receptor Rev-erb alpha regulates circadian expression of plasminogen activator inhibitor type 1. *J. Biol. Chem.* **281,** 33842–33848
49. Cho, H., Zhao, X., Hatori, M., Yu, R. T., Barish, G. D., Lam, M. T., Chong, L. W., DiTacchio, L., Atkins, A. R., Glass, C. K., Liddle, C., Auwerx, J., Downes, M., Panda, S., and Evans, R. M. (2012) Regulation of circadian behaviour and metabolism by REV-ERB-alpha and REV-ERB-beta. *Nature* **485,** 123–127
50. Botelho, R. J., Harrison, R. E., Stone, J. C., Hancock, J. F., Philips, M. R., Jongstra-Bilen, J., Mason, D., Plumb, J., Gold, M. R., and Grinstein, S. (2009) Localized diacylglycerol-dependent stimulation of Ras and Rap1 during phagocytosis. *J. Biol. Chem.* **284,** 28522–28532
51. Almena, M., and Merida, I. (2011) Shaping up the membrane: diacylglycerol coordinates spatial orientation of signaling. *Trends Biochem. Sci.* **36,** 593–603
52. Botelho, R. J., Teruel, M., Dierckman, R., Anderson, R., Wells, A., York, J. D., Meyer, T., and Grinstein, S. (2000) Localized biphasic changes in phosphatidylinositol-4,5-bisphosphate at sites of phagocytosis. *J. Cell Biol.* **151,** 1353–1367
53. Ding, L., Traer, E., McIntyre, T. M., Zimmerman, G. A., and Prescott, S. M. (1998) The cloning and characterization of a

novel human diacylglycerol kinase, DGK iota. *J. Biol. Chem.* **273,** 32746–32752
54. Kolko, M., Wang, J. M., Zhan, C., Poulsen, K. A., Prause, J. U., Nissen, M. H., Heegaard, S., and Bazan, N. G. (2007) Identification of intracellular phospholipases A(2) in the human eye: Involvement in phagocytosis of photoreceptor outer segments. *Invest. Ophth. Vis. Sci.* **48,** 1401–1409
55. Strunnikova, N. V., Maminishkis, A., Barb, J. J., Wang, F., Zhi, C., Sergeev, Y., Chen, W., Edwards, A. O., Stambolian, D., Abecasis, G., Swaroop, A., Munson, P. J., and Miller, S. S. (2010) Transcriptome analysis and molecular signature of human retinal pigment epithelium. *Hum. Mol. Genet.* **19,** 2468–2486
56. Shelby, S. J., Colwill, K., Dhe-Paganon, S., Pawson, T., and Thompson, D. A. (2013) MERTK interactions with SH2-domain proteins in the retinal pigment epithelium. *PLoS One* **8,** e53964
57. Green, C. B., Takahashi, J. S., and Bass, J. (2008) The meter of metabolism. *Cell* **134,** 728–742
58. Hughes, M. E., Grant, G. R., Paquin, C., Qian, J., and Nitabach, M. N. (2012) Deep sequencing the circadian and diurnal transcriptome of *Drosophila* brain. *Genome Res.* **22,** 1266–1281
59. Tovin, A., Alon, S., Ben-Moshe, Z., Mracek, P., Vatine, G., Foulkes, N. S., Jacob-Hirsch, J., Rechavi, G., Toyama, R., Coon, S. L., Klein, D. C., Eisenberg, E., and Gothilf, Y. (2012) Systematic identification of rhythmic genes reveals camk1gb as a new element in the circadian clockwork. *PLoS Genetics* **8,** e1003116
60. Ruggiero, L., Connor, M. P., Chen, J., Langen, R., and Finnemann, S. C. (2012) Diurnal, localized exposure of phosphatidylserine by rod outer segment in wild-type but not Itgb5(-/-) or Mfge8(-/-) mouse retina. *Proc. Natl. Acad. Sci. U. S. A.* **109,** 8145–8148
61. Finnemann, S. C., Bonilha, V. L., Marmorstein, A. D., and RodriguezBoulan, E. (1997) Phagocytosis of rod outer segments by retinal pigment epithelial cells requires alpha v beta 5 integrin for binding but not for internalization. *Proc. Natl. Acad. Sci. U. S. A.* **94,** 12932–12937
62. Ryeom, S. W., Sparrow, J. R., and Silverstein, R. L. (1996) CD36 participates in the phagocytosis of rod outer segments by retinal pigment epithelium. *J. Cell Sci.* **109,** 387–395
63. Crandall, D. L., Busler, D. E., McHendry-Rinde, B., Groeling, T. M., and Kral, J. G. (2000) Autocrine regulation of human preadipocyte migration by plasminogen activator inhibitor-1. *J. Clin. Endocrinol. Metab.* **85,** 2609–2614
64. Nandrot, E. E., Kim, Y. H., Brodie, S. E., Huang, X. Z., Sheppard, D., and Finnemann, S. C. (2004) Loss of synchronized retinal phagocytosis and age-related blindness in mice lacking alpha v beta 5 integrin. *J. Exp. Med.* **200,** 1539–1545
65. Jeon, H., Kim, J. H., Kim, J. H., Lee, W. H., Lee, M. S., and Suk, K. (2012) Plasminogen activator inhibitor type 1 regulates microglial motility and phagocytic activity. *J. Neuroinflammation* **9,** 149
66. Park, Y. J., Liu, G., Lorne, E. F., Zhao, X., Wang, J., Tsuruta, Y., Zmijewski, J., and Abraham, E. (2008) PAI-1 inhibits neutrophil efferocytosis. *Proc. Natl. Acad. Sci. U. S. A.* **105,** 11784–11789
67. Burstyn-Cohen, T., Lew, E. D., Traves, P. G., Burrola, P. G., Hash, J. C., and Lemke, G. (2012) Genetic dissection of TAM receptor-ligand interaction in retinal pigment epithelial cell phagocytosis. *Neuron* **76,** 1123–1132
68. Finnemann, S. C. (2003) Focal adhesion kinase signaling promotes phagocytosis of integrin-bound photoreceptors. *EMBO J.* **22,** 4143–4154
69. Todt, J. C., Hu, B., and Curtis, J. L. (2004) The receptor tyrosine kinase MerTK activates phospholipase C gamma 2 during recognition of apoptotic thymocytes by murine macrophages. *J. Leukoc. Biol.* **75,** 705–713
70. Posor, Y., Eichhorn-Gruenig, M., Puchkov, D., Schoneberg, J., Ullrich, A., Lampe, A., Muller, R., Zarbakhsh, S., Gulluni, F., Hirsch, E., Krauss, M., Schultz, C., Schmoranzer, J., Noe, F., and Haucke, V. (2013) Spatiotemporal control of endocytosis by phosphatidylinositol-3,4-bisphosphate. *Nature* **499,** 233–237
71. Steinckwich, N., Schenten, V., Melchior, C., Brechard, S., and Tschirhart, E. J. (2011) An essential role of STIM1, Orai1, and S100A8-A9 proteins for Ca(2+) signaling and Fc gamma R-mediated phagosomal oxidative activity. *J. Immunol.* **186,** 2182–2191
72. Berridge, M. J., Bootman, M. D., and Roderick, H. L. (2003) Calcium signalling: dynamics, homeostasis and remodelling. *Nat. Rev. Mol. Cell Biol.* **4,** 517–529
73. Swanson, J. A. (2008) Shaping cups into phagosomes and macropinosomes. *Nat. Rev. Mol. Cell Biol.* **9,** 639–649
74. Carrasco, S., and Merida, I. (2004) Diacylglycerol-dependent binding recruits PKC theta and RasGRP1 C1 domains to specific subcellular localizations in living T lymphocytes. *Mol. Biol. Cell* **15,** 2932–2942
75. Lorenzo, P. S., Beheshti, M., Pettit, G. R., Stone, J. C., and Blumberg, P. M. (2000) The guanine nucleotide exchange factor RasGRP is a high-affinity target for diacylglycerol and phorbol esters. *Mol. Pharmacol.* **57,** 840–846
76. Regier, D. S., Higbee, J., Lund, K. M., Sakane, F., Prescott, S. M., and Topham, M. K. (2005) Diacylglycerol kinase iota regulates Ras guanyl-releasing protein 3 and inhibits Rap1 signaling. *Proc. Natl. Acad. Sci. U. S. A.* **102,** 7595–7600
77. Huynh, K. K., Eskelinen, E. L., Scott, C. C., Malevanets, A., Saftig, P., and Grinstein, S. (2007) LAMP proteins are required for fusion of lysosomes with phagosomes. *EMBO J.* **26,** 313–324
78. Araki, N., Johnson, M. T., and Swanson, J. A. (1996) A role for phosphoinositide 3-kinase in the completion of macropinocytosis and phagocytosis by macrophages. *J. Cell Biol.* **135,** 1249–1260
79. Glaser, M., Wanaski, S., Buser, C. A., Boguslavsky, V., Rashidzada, W., Morris, A., Rebecchi, M., Scarlata, S. F., Runnels, L. W., Prestwich, G. D., Chen, J., Aderem, A., Ahn, J., and McLaughlin, S. (1996) Myristoylated alanine-rich C kinase substrate (MARCKS) produces reversible inhibition of phospholipase C by sequestering phosphatidylinositol 4,5-bisphosphate in lateral domains. *J. Biol. Chem.* **271,** 26187–26193
80. Allen, L. A. H., and Aderem, A. (1995) A role for Marcks, the alpha-isozyme of protein-kinase-C and myosin-I in zymosan phagocytosis by macrophages. *J. Exp. Med.* **182,** 829–840
81. Van den Bout, I., Truong, H. H., Huveneers, S., Kuikman, I., Danen, E. H. J., and Sonnenberg, A. (2007) The regulation of MacMARCKS expression by integrin beta 3. *Exp. Cell Res.* **313,** 1260–1269
82. Rey, G., Cesbron, F., Rougemont, J., Reinke, H., Brunner, M., and Naef, F. (2011) Genome-wide and phase-specific DNA-binding rhythms of BMAL1 control circadian output functions in mouse liver. *PLoS Biol.* **9,** e1000595
83. Vollmers, C., Schmitz, R. J., Nathanson, J., Yeo, G., Ecker, J. R., and Panda, S. (2012) Circadian oscillations of protein-coding and regulatory RNAs in a highly dynamic mammalian liver epigenome. *Cell Metab.* **16,** 833–845
84. Mustafi, D., Kevany, B. M., Bai, X., Maeda, T., Sears, J. E., Khalil, A. M., and Palczewski, K. (2013) Evolutionarily conserved long intergenic non-coding RNAs in the eye. *Hum. Mol. Genet.* **22,** 2992–3002
85. Koike, N., Yoo, S. H., Huang, H. C., Kumar, V., Lee, C., Kim, T. K., and Takahashi, J. S. (2012) Transcriptional architecture and chromatin landscape of the core circadian clock in mammals. *Science* **338,** 349–354
86. Alenghat, T., Meyers, K., Mullican, S. E., Leitner, K., Adeniji-Adele, A., Avila, J., Bucan, M., Ahima, R. S., Kaestner, K. H., and Lazar, M. A. (2008) Nuclear receptor corepressor and histone deacetylase 3 govern circadian metabolic physiology. *Nature* **456,** 997–1000
87. Gregory, G. D., Vakoc, C. R., Rozovskaia, T., Zheng, X., Patel, S., Nakamura, T., Canaani, E., and Blobel, G. A. (2007) Mammalian ASH1L is a histone methyltransferase that occupies the transcribed region of active genes. *Mol. Cell. Biol.* **27,** 8466–8479
88. Zhang, E. E., Liu, A. C., Hirota, T., Miraglia, L. J., Welch, G., Pongsawakul, P. Y., Liu, X., Atwood, A., Huss, J. W., 3rd, Janes, J., Su, A. I., Hogenesch, J. B., and Kay, S. A. (2009) A genome-wide RNAi screen for modifiers of the circadian clock in human cells. *Cell* **139,** 199–210

Received for publication June 18, 2013.
Accepted for publication July 22, 2013.